water

MDPI

Article

Projected Changes in Hydrological Variables in the Agricultural Region of Alberta, Canada

Mohammad Badrul Masud, Jannatul Ferdous and Monireh Faramarzi *

Watershed Science and Modelling Laboratory, Department of Earth and Atmospheric Sciences, University of Alberta, Edmonton, AB T6G 2R3, Canada; masud@ualberta.ca (M.B.M.); jannatul@ualberta.ca (J.F.)

* Correspondence: faramarz@ualberta.ca; Tel.: +1-780-492-7241

Received: 19 November 2018; Accepted: 6 December 2018; Published: 9 December 2018

Abstract: The responses of regional hydrological variables to climate change are of prime concern for agricultural water resources planning and management. Therefore, the seasonal (April–September) and annual (January–December) evolution of precipitation, temperature, evapotranspiration (ET), soil moisture (SM), deep aquifer recharge (DA), and water yield (WYLD) was investigated using established statistical techniques for the historical, near and far future (1983–2007: His, 2010–2034: NF, 2040–2064: FF) in the agricultural region of Alberta, Canada. Previously calibrated and validated agro-hydrological models (Soil and Water Assessment Tool) were used to generate these variables. Future changes were investigated under two representative concentration pathways, i.e., RCP 2.6 and RCP 8.5, projected by nine global climate models (GCM). Results revealed that Alberta had become warmer and drier during the His period. The future projection showed an increase in precipitation, SM, DA, and WYLD, in turn, indicated more water resources. Precipitation and temperature were projected to increase between 1 to 7% and 1.21 to 2.32 °C, respectively. Seasonal precipitation showed a higher trend magnitude than that of annual precipitation. The temperature generally had an increasing trend in the future with a maximum in the southern Alberta. Monthly average ET was likely to increase and decrease in the rising and falling limbs of the bell-shaped curve with the peak in July. A comparison of water demand from two land use types (dominant land use and barley) during the His period showed that water deficit existed in July and August. The results of this study could help in understanding anticipated changes in hydrological variables and decision-making regarding the regional agricultural water resources management.

Keywords: hydrologic modelling; SWAT; climate variability; trend detection; modified Mann–Kendall test; Sen's slope estimator; climate change

1. Introduction

Global climate warming is undoubtedly happening due to the anthropogenic actions which include burning fossil fuels, deforestation and rapid urbanization [1]. It modifies the intensity and frequency of precipitation, in turn, changes the hydrological cycle. This change is likely to increase in the future [2] and will continue to pose a threat to the water availability for different sectors, e.g., agriculture [3]. Soil water availability in an agricultural region is one of the primary inputs to raise agricultural production to feed a growing world population. Precipitation is a key driver controlling soil water in most of the rainfed croplands, whereas temperature is particularly important in most snow-dominated and semi-arid areas [3] as in Canada. The sensitivity of semi-arid regions to changes in precipitation and temperature increases regional vulnerability to potential effects of climate change on water resources and agriculture. Therefore, it is essential to investigate the changing properties of agro-hydrological variables including precipitation, temperature, evapotranspiration, soil water, deep aquifer recharge, and water yield due to climate change.

Many studies have focused on analyzing precipitation and temperature trends over a range of geographic regions [4–6] across the world. With respect to temperature, the overall trend at the global scale shows uniformly increasing, while it is less uniform at smaller spatiotemporal scales. For example, the surface and ocean global mean annual temperature increased by 0.85 ± 0.21 °C over 1880 to 2012 period [3]. On the other hand, the mean annual temperature in Turkey and Eastern China increased by 0.88 and 1.52 °C, respectively [7,8]. Relative to temperature, precipitation is highly characterized by spatial variability, and it is dependent on regional and local variables. Philandras et al. [9] found the annual precipitation within the Mediterranean region was generally negative over the 1901–2009 period, while Machiwal et al. [10] found the opposite in an arid region in India. Vincent et al. [11] investigated Canada-wide annual mean surface air temperature and found an increase of 1.5 °C over the 1950 to 2010 period. This warming is accompanied by changes in other variables including a mixture of non-significant positive and negative trends in seasonal precipitation of Canadian prairies [12] and decreases in streamflow [13]. In such cases of high variability in changes, the relatively small-scale analysis may be helpful in practical applications [6]. Despite temperature and precipitation that have been focus of an overwhelming majority of trend studies in literature, limited research is available on trend analysis of evapotranspiration, soil moisture, deep aquifer recharge, and water yield [14]. These variables profoundly influence the hydrological cycle in the context of climate change and agricultural productivity. Therefore, a study of trend analysis of these variables would provide a comprehensive understanding of water resources availability and will help to frame better water resource management.

Hydrologic models have gained widespread attention to understand the implication of climate change on water availability. The Soil and Water Assessment Tool (SWAT) has widely been used to assess the impact of climate change on hydrological variables [15,16], water resources [17], and water balance components [18]. For instance, Mehan et al. [18] used the SWAT model to examine the impact of climate change on the hydrological processes in a small agricultural watershed in South Dakota. The model was also used to evaluate the impacts of changes in precipitation, temperature and CO_2 concentration on water resources in Spain [19].

This study investigates the variability and trend of hydrological variables, i.e., precipitation, temperature, evapotranspiration, soil moisture, deep aquifer recharge and water yield under the impacts of climate change in Alberta, Canada. The province of Alberta was considered as a case study since it is an important agricultural region in Canada and food supplier for the world. The province encompasses 17 main river basins with each including diverse agro-hydrologic and hydro-climatic conditions. An extensive calibration and validation of hydrologic models of Alberta are available [20,21], allowing simulation of agro-hydrologic variables for the purpose of this study.

2. Methodology

2.1. Study Area

Alberta is located between 45° N to 65° N and 105° E to 125° E in the semi-arid Canadian Prairies with the area of about 660,000 km^2, where altitude varies from 152 to 3747 m above the mean sea level (Figure 1). The annual precipitation of Alberta is 482 mm, and provincial average precipitation in summer is 200–300 mm [21]. Precipitation ranges from 400 mm (northeast) to over 500 mm on the northwest, and it ranges from ~350 mm (southeast) to about 450 mm (southwest) in southern areas. The mean maximum and minimum annual air temperature is 8.4 °C and −4 °C and it is 25.5 and 10.5 °C in summer, respectively [21]. The study area has four distinct seasons: summer (June–August), fall (September–November), winter (December–February), and spring (March–May).

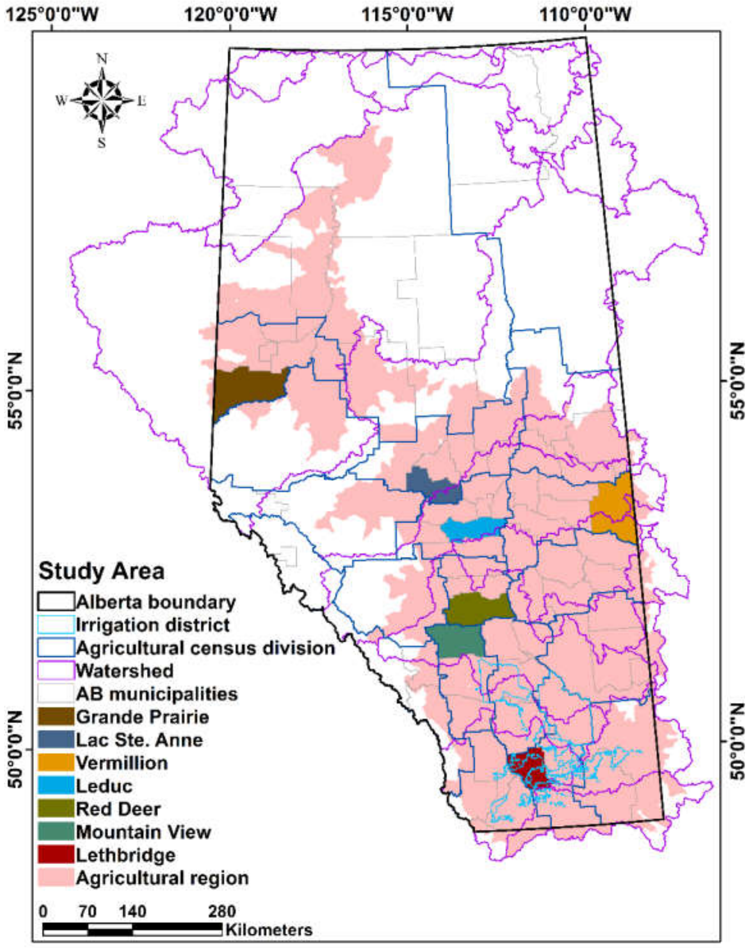

Figure 1. Map of the study area (agricultural region) overlaid with the Alberta boundary, watersheds, agricultural census divisions, Alberta municipalities and irrigation districts of Alberta. The seven shaded areas are the location of case study for trend analysis.

The province has 17 river basins and 19 census divisions (CD) of agriculture with 43,234 agricultural farms. The agricultural region of Alberta is spread out in 11 out of 17 river basins (Figure 1) that are chosen to assess the spatial variability of hydrological parameters in this study. A total of seven counties from seven agricultural CD were selected based on the number of farms for trend analysis (Table 1). First, the CD with the total number of farms in the division more than 2000 was selected. Next, the county in each CD with a total number of farms >900 was selected for trend analysis. No county had been selected having less than 900 farms, even if the CD had more than 2000 farms (Table 1). The name of these counties are-(a) Grande Prairie from Grande Prairie CD, (b) LacStAnne from Barrhead/Athabasca CD, (c) Leduc from Edmonton CD, (d) Lethbridge from Lethbridge CD, (e) Mountain View from Calgary CD, (f) Red Deer from Red Deer CD, and (g) Vermilion from Camrose/Vermilion CD (Figure 1). The selected counties represent various hydro-climate, geospatial, and management conditions in the province's agricultural lands.

Based on the best available land use–land cover map (see Section 2.3), the dominant land use types were different across counties. For example, Agricultural Land-Row Crops (AGRR) and Forest-Deciduous (FRSD) land use types were found to be dominant in the Grande Prairie county, whereas Pasture (PAST) and Spring Wheat (SWHT) were considered as the main land use types in LacStAnne, Leduc and Lethbridge County, respectively (Table 1). The dominant land use type in the rest of the counties were AGRR. The overall dominant land use type in the agricultural region of Alberta was AGRR followed by FRSD.

Table 1. Number of farms in seven counties, identified by their census divisions, and selected as case study-2011 Census of Agriculture.[1]

Census Division (CD)	# Farms in the CD	County (# Farms >900)	# Farms in the Country	Dominant Land Use *
CD 2. Lethbridge	2790	Lethbridge	933	SWHT
CD 6. Calgary	4186	Mountain View	1636	AGRR
CD 8. Red Deer	3682	Red Deer	1531	AGRR
CD 10. Camrose/Vermilion	4616	Vermilion River	1029	AGRR
CD 11. Edmonton	5034	Leduc	1255	PAST
CD 13. Barrhead/Athabasca	3833	Lac Ste. Anne	936	PAST
CD 19. Grande Prairie/Fairview	2734	Grande Prairie	1206	AGRR & FRSD

* AGRR-Agricultural Land-Row Crops; PAST-Pasture; FRSD-Forest-deciduous; SWHT-Spring wheat. [1] Source: Adopted from Agriculture Statistics Yearbook 2013 (http://www1.agric.gov.ab.ca/$department/deptdocs.nsf/all/sdd15054/$file/2013-yearbook.pdf).

2.2. Data Collection

The study period was divided into three different time horizons (a) historical (His: 1983 to 2007), (b) near future (NF: 2010 to 2034), and (c) far future (FF: 2040 to 2064). The climate data were collected from 300 meteorological stations at a daily time step from Environment and Climate Change Canada (http://climate.weather.gc.ca/) for His period. For NF and FF, climate change data for nine Global Climate Models (GCMs) namely-CanESM2, CCSM4, CNRM-CM5, CSIRO-MK3, GFDL-ESM2G, HADGEM2, MIROC5, MPI-ESMLR, and MRI-CGCM3, were collected from the Pacific Climate Impacts Consortium (PCIC; https://www.pacificclimate.org/data) under two RCP scenarios, i.e., RCP 2.6 and 8.5. The selected GCMs are the best model combination out of the majority of IPCC collection that represents the largest plausible future in Canada [22]. The calibrated hydrological model [20,23] was used to simulate hydrologic water balance variables for each climate model and scenario. Owing to uncertainties in the detailed representation of many complex climate processes, individual climate models vary in their representation of these processes and will have biases of various kinds [24]. Hence, it is suggested to use multi-model ensemble average of projections, which produces smaller errors than any individual model [24,25]. Therefore, results of this study were presented as the ensemble average of nine GCMs in this study. In this study, months from April to September were considered to explain the results in 'seasonal' scale, whereas January to December was considered for the 'annual' scale.

2.3. The SWAT Model

The Soil and Water Assessment Tool (SWAT) is a physical process-based, time-continuous hydrological model [26]. This model simulates hydrological variables within small or large watersheds under different management, land use change, and climate change scenarios for impact assessment. Based on topographic data, soil characteristics and land use type, the model delineates watersheds into unique spatial units and predicts future hydrological variables using a water balance equation in each unit (Figure 2) [27]:

$$SW_t = SW_0 + \sum_{i=1}^{t}\left(R_{day} - Q_{surf} - E_a - w_{seep} - Q_{gw}\right) \quad (1)$$

where, SW_t = final soil water content (mm); SW_0 = initial soil water content on day i (mm); t = time (days); R_{day} = amount of precipitation on day i (mm); Q_{surf} = amount of surface runoff on day i (mm); E_a = amount of evapotranspiration on day i (mm); w_{seep} = amount of water entering the vadose zone from the soil profile on day i (mm); Q_{gw} = amount of return flow on day i (mm).

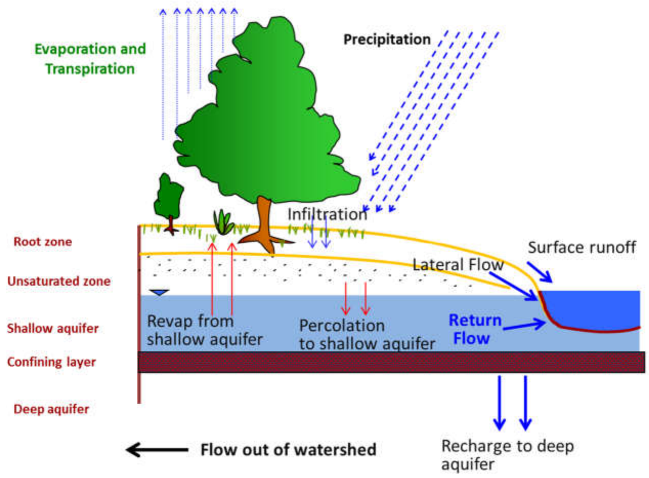

Figure 2. Hydrological cycle in the Soil and Water Assessment Tool (SWAT) model (adopted from SWAT model manual).

The SWAT model also simulates potential evapotranspiration (PET). Three methods have incorporated into SWAT including the Penman–Monteith, Priestley–Taylor and Hargreaves method to calculate PET. We used the Penman–Monteith method as follow [28]:

$$\lambda E = \frac{\Delta \cdot (H_{net} - G) + \rho_{air} \cdot c_p \cdot [e_z^o - e_z]/r_a}{\Delta + \gamma \cdot (1 + r_c/r_a)} \quad (2)$$

where λE is the latent heat flux density (MJ m^{-2} d^{-1}), E is the depth rate of evaporation (mm day^{-1}), Δ is the slope of the saturation vapor pressure-temperature curve, de/dt (kPa °C^{-1}), H_{net} is the net radiation (MJ m^{-2} day^{-1}), G is the heat flux density to the ground (MJ m^{-2} day^{-1}), ρ_{air} is the air density (kg m^{-3}), c_p is the specific heat at constant pressure (MJ kg^{-1} °C^{-1}), e_z^o is the saturation vapor pressure of air at height z (kPa), e_z is the water vapor pressure of air at height z (kPa), γ is the psychrometric constant (kPa °C^{-1}), r_c is the plant canopy resistance (s m^{-1}), and r_a is the diffusion resistance of the air layer (aerodynamic resistance) (s m^{-1}). The model simulates actual evapotranspiration (AET) based on PET, soil water availability, and the maximum amount of transpiration depending on the plant type and related daily above-ground and below-ground biomass production. This AET is used in this study and referred to evapotranspiration (ET) afterward.

The model works on the concept that the daily precipitation can generate surface runoff, and a fraction can infiltrate into the soil depending on land use and soil characteristics. Further, a fraction of daily soil water becomes available for plant evapotranspiration. It will also partition into a subsurface flow to stream and recharge to the shallow aquifer that will partially feed streamflow. The recharge can be routed to the deep aquifer. The amount of water will be diverted from the shallow aquifer due to percolation to the deep aquifer is the total recharge entering the aquifer multiplied by the aquifer percolation coefficient. The water yield in the SWAT model is the amount of water leaving a hydrologic response unit and entering the main channel during the simulated time-step. For more details see Neitsch et al. [28].

The model was built using the digital elevation model at 10-m resolution [29], land use-land cover maps and related physical parameters (http://www.geobase.ca/geobase/en/data/landcover/csc2000v/description.html) and soil map with the soil physical properties embodied in the map (http://sis.agr.gc.ca/cansis/nsdb/slc/index.html) as well as agro-hydrological data [20,23]. A total of 2255 sub-basins were delineated for Alberta [23], however, in this study we extracted the sub-basins that are located within the agricultural region. An extensive calibration and validation of the hydrologic and crop models were conducted [20,21,23]. Two statistical measures were used to quantify the goodness-of-fit and model output uncertainty using the Sequential Uncertainty Fitting (SUFI-2) program. The SUFI-2 program is linked to SWAT and provides the basis for parallel processing of calibration and large-scale parameterization schemes [20,21,23]. Two statistical measures are p-factor, which is the percentage of observed data bracketed by the model outputs uncertainty, quantified as 95% prediction uncertainty (95PPU), and r-factor, which is the average thickness of the 95PPU band, were used to check the model performance during calibration and validation. The 95PPU is calculated at 2.5% and 97.5% levels of the cumulative distribution of an output variable [20,21,23]. The r-factor is the average width of the 95PPU band divided by the standard deviation of the observed variable. In an ideal condition, a p-factor of hundred percent and r-factor of zero is the simulation that exactly brackets the observed data. Calibrated-validated models were used to simulate historical and future water balance components for further analysis in this study.

2.4. Assessment of Hydrological Variables

Simulated daily records of agro-hydrological variables (temperature, precipitation, evapotranspiration, soil moisture, deep aquifer recharge, and water yield) were aggregated into seasonal (April–September) and annual (January–December) means. Long-term monthly mean also used to examine monthly changes in hydrological variables. Long-term mean has been used by hydrologists and climatologists in different regions of the world [30,31].

2.5. Trends of Hydrological Variables

A variety of statistical methods can detect the trends of hydrological variables at different temporal scale. Both non-parametric (Mann–Kendall test) [32,33] and parametric (linear regression analysis) procedures are used to identify the annual and seasonal trends. The Mann–Kendall (MK) statistical test is used worldwide to detect the trend of precipitation, temperature, and relative humidity [14,34–37]. The non-parametric tests are preferred as they are more suitable for non-normally distributed data, which are frequently encountered in hydro-meteorological time series [38]. Although the original MK test has been widely used and recommended by the World Meteorological Organization, it fails to deal with the issue of autocorrelation in the hydro-meteorological time series. Hamed and Rao [38] improved the MK test by taking the lag-*i* autocorrelation into consideration; and the modified MK (MMK) has been shown to be robust in capturing the trends of the hydro-meteorological time series [39]. Chen et al. [15] also found that the MMK test's performance is better than the original MK test if data is autocorrelated. In this study, the trend obtained by the MMK test was assessed at the significance level of $\alpha = 5\%$.

In addition to the trend detection, it is necessary to estimate the trend magnitude. Sen's nonparametric method [38] is used to estimate the true slope of an existing trend (as change per year). Sen's slope method gives a robust estimation of the trend and is used in various trend analyses of hydrological variables [38]. Hence, the non-parametric statistical trend analysis is recommended to assess the impact of climate change on the hydrological variables. A $100\ (1-\alpha)\%$ two-sided confidence interval about the slope estimate is obtained by the nonparametric technique based on the normal distribution. A positive value of trend estimation indicates an upward trend and a negative value indicates a downward trend in the time series.

2.6. Potential Land Use Type and Water Source

The ET was simulated by SWAT agro-hydrologic models for dominant land use (ET_DLU) and barley crop (ET_barley) for His period [20,21]. These two ET were used for comparison of the water demand differences in a county for two land use types. We intended to get a sense of how large the water demand of current dominant land use type is in a county as compared to a potential crop type. We also calculated water deficit (WD) for His period by taking the difference between precipitation and ET for each land use type (ET_DLU and ET_barley). The WD can provide useful information on how the water needs of an existing land use type are compensated by precipitation. For example, in a given county, large negative delta (i.e., precipitation minus ET) for a given land use type indicates that the plant water needs were from either irrigation or other sources than the natural soil water from precipitation.

3. Results

3.1. The SWAT Model Performance

We used outputs from the SWAT hydrological and crop simulation models in this study. A multi-gauge and multi-objective calibration using river discharges and crop yield ensured proper apportioning of precipitation and soil water into surface runoff, actual evapotranspiration, and groundwater recharge. Altogether, measured discharge data of 130 hydrometric stations and annual yield data of 67 counties were used to calibrate and validate the agro-hydrologic model. The model performance was satisfactory for most of the hydrometric stations and counties. Overall, 63% and 71% of the observed streamflow data, and 88% and 85% of observed crop yield data were captured by the model uncertainty prediction for calibration and validation periods, respectively. The average r-factor was about 1.04 and 1.43 for discharge and 4.48 and 5.35 for crop yields during the calibration and validation, respectively at the Alberta scale (Table 2). For yield simulation in the best performing counties, the model captured 79% of observed data with an r-factor of 2.51, while the model captured 95% of observed data with an r-factor of 6.85 in the worst case. Larger r-factor in the crop model might be due to climate variability and unreliable precipitation distribution in Alberta, and this has increased standard deviation as well as the thickness of the uncertainty band. Detailed performance results of the hydrological and crop simulation models can be found in Faramarzi et al. [20] and Masud et al. [21], respectively.

Table 2. Performance statistics for the SWAT hydrological and SWAT crop simulation models at the provincial scale.

Hydrological Model			
Calibration		Validation	
p-factor (%)	r-factor	p-factor (%)	r-factor
63	1.04	71	1.43
Crop Model			
Calibration		Validation	
p-factor (%)	r-factor	p-factor (%)	r-factor
88	4.48	85	5.35

3.2. Seasonal and Annual Variation of Hydrological Variables

We examined seasonal and annual changes of hydrological variables for the agricultural region of Alberta. The study was performed for the historical (1983–2007) and future (2010–2064) periods projected by nine GCMs under two RCP scenarios. In this section, we presented and discussed results based on the ensemble average of all GCMs.

Figure 3 shows historical and projected future seasonal and annual precipitation distribution. Historical precipitation distribution showed that southeastern part was drier than any other area of the agricultural region. The precipitation was high in the west and followed by the central part of the region. Annual and seasonal precipitation ranged from 280 to 745 mm and 208 to 493 mm, respectively. Projected changes in annual and seasonal precipitation in both NF and FF indicated a likely increase compare to the His, which was higher for FF followed by NF. Most of the sub-basins were likely to gain higher precipitation during NF as compared to His, while some of them were likely to receive less precipitation. In the FF, precipitation was projected to increase uniformly over the study area having a maximum in the eastern part.

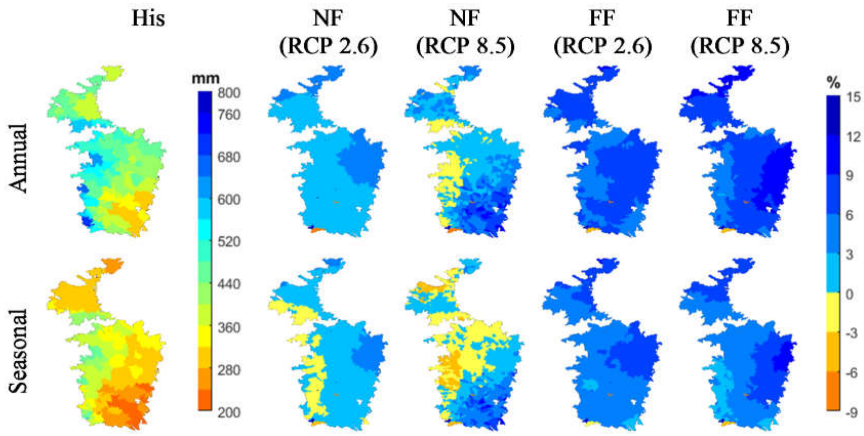

Figure 3. Spatial distribution of mean seasonal and annual precipitation and their projected changes (%) in the future under RCP 2.6 and 8.5, where His indicates historical period (1983–2007), NF indicates near future (2010–2034) and FF indicates far future (2040–2064).

Annual precipitation was projected to increase by 3% and 7% in most of the sub-basins during the NF and FF. Similarly, the seasonal precipitation could increase by 1% and 5% for two future horizons. It is worth to mention that projected increase in southern sub-basins will not result in a significant amount of precipitation since the historical precipitation is minimum in this area.

The variation of seasonal and annual mean temperature is presented in Figure 4, and the maximum and minimum temperature maps are shown in the Supplementary Materials (Figures S1 and S2). The southern region was hotter with the lowest amount of precipitation for all periods while the northwestern part was colder with the highest amount of precipitation. The average annual mean, maximum, and minimum temperatures were found to be 5, 9, and −0.2 °C during the His period. Likewise, the average seasonal mean, maximum, and minimum temperatures were found to be 13, 19, and 7 °C. Compare to the His period, the temperature was rising in NF and FF with a maximum increase in FF (Figure 4). The spatial distribution of the temperature rise was different for the annual and seasonal case. The largest temperature increase was projected for the eastern and southern part of the region for the annual and seasonal case, respectively. In general, the average rise of mean annual and the seasonal temperature was 1.33 and 1.21 °C in NF, while it was 2.32 and 2.14 °C in FF, respectively. The spatial patterns of maximum and minimum temperature for His and projected changes for the NF and FF were similar to the spatial pattern of mean temperature. This GCM projected precipitation and temperature changes agreed with previous studies [40–44]. These results are also supported by the recent results reported by Environment and Climate Change Canada [24] in a country-wide study.

The spatial distribution of ET and soil moisture (SM) is shown in Figures 5 and 6. The projection suggested larger increase (decrease) in ET (SM) in the sub-basins, where the temperature was also projected to increase with high precipitation. These findings are in agreement with some small-scale studies in southern Alberta [41,43,45]. Spatial distribution of deep aquifer recharge and water yield is shown in the Supplementary Materials (Figures S3 and S4). According to Falkenmark and Rockstrom [46], the summation of water yield (WYLD) and deep aquifer recharge (DA) is termed as blue water. The spatial pattern of blue water components was similar to that of precipitation. Out of the 440-mm mean annual precipitation in His period, about 64 mm was renewable blue water resources in the agricultural region. Based on the projected changes, the blue water resources were expected to marginally increase in most of the sub-basins.

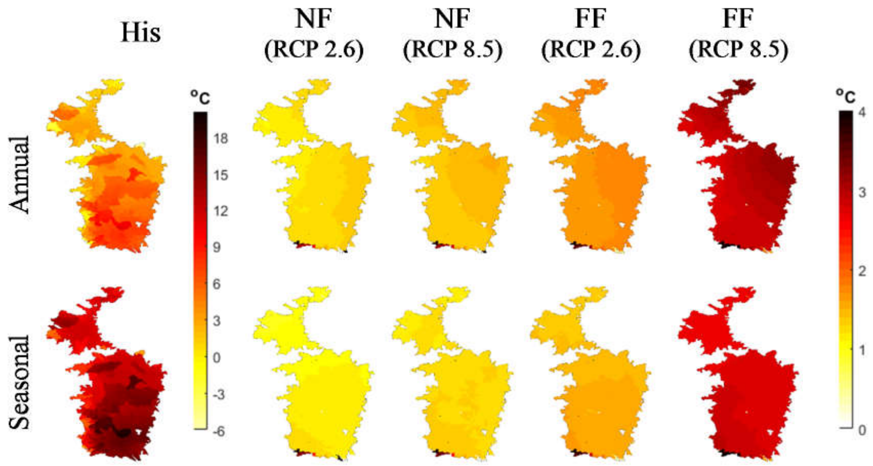

Figure 4. Spatial distribution of mean seasonal and annual temperature and their projected changes (°C) in the future under RCP 2.6 and 8.5, where His indicates historical period (1983–2007), NF indicates near future (2010–2034) and FF indicates far future (2040–2064).

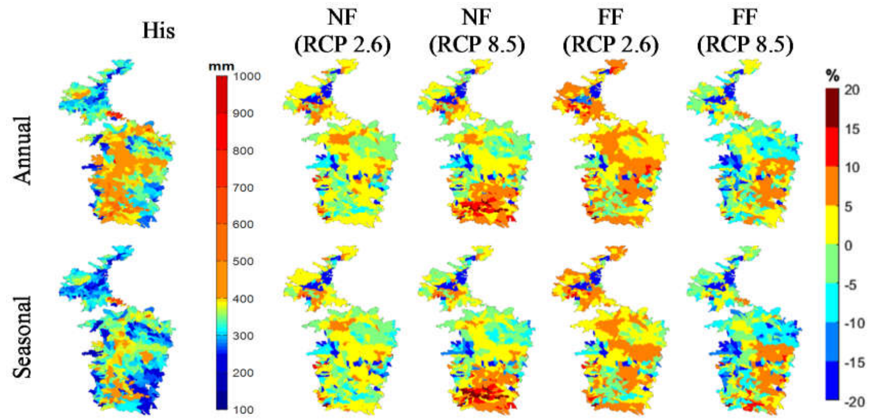

Figure 5. Spatial distribution of ET by RCP (representative concentration pathway) 2.6 and 8.5, where His indicates historical period (1983–2007), NF indicates near future (2010–2034) and FF indicates far future (2040–2064). For historical period simulated ET is shown in the map, and for the NF and FF percentage change is shown in the map.

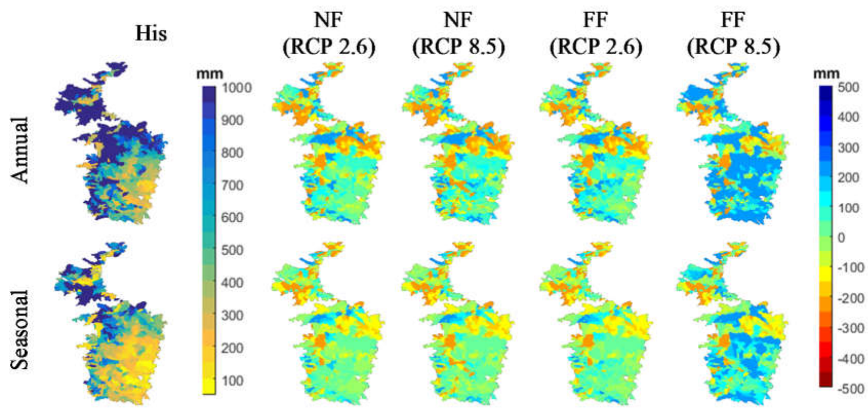

Figure 6. Spatial distribution of soil moisture by RCP 2.6 and 8.5, where His indicates historical period (1983–2007), NF indicates near future (2010–2034) and FF indicates far future (2040–2064). For historical period simulated soil moisture is shown in the map, and for the NF and FF difference of soil moisture is shown in the map.

3.3. Seasonal and Annual Trends of Hydrological Variables

Trend of seasonal and annual precipitation and temperature were analyzed for the current and future periods. The magnitude of the trend and its significance in the time series were determined using the Sen's slope estimator and the MMK test (Table 3). The trend analysis was performed separately for RCP 2.6 and 8.5 in seven selected counties (Table 1) in the Alberta agricultural region for His, NF and FF.

During His period, annual and seasonal precipitation showed a decreasing trend in all counties, except in Lethbridge and Red Deer, where seasonal precipitation showed an increasing trend (Table 3). However, Grande Prairie county only observed the statistically significant negative trend. Likewise, non-significant positive and negative annual trends were found for NF and FF, which was similar to the His period in most of the counties. Only Grande Prairie observed a statistically significant negative trend in NF for RCP 2.6. In general, seasonal precipitation showed an upward or downward trend with a higher magnitude than annual precipitation for both RCPs.

The trend magnitude of both annual and seasonal mean temperature varied slightly among different counties, and it ranged from 0.03–0.05 °C (annual) and 0.01–0.02 °C (seasonal). Table 3 also indicated that the trend of mean temperature generally increased from southern to northern Alberta. In other words, the region with lower mean temperature (Figure 4) in His period had a higher warming rate in the future. The increasing trend of mean temperature was observed in the NF and FF. However, most of the counties showed non-significant trend except Mountain View, where the trend was found to be significant. The trend magnitude of annual mean temperature was usually higher than the seasonal mean temperature. Similar trends were found for both maximum and minimum temperature for the historical as well as future periods (Table 3). Jiang et al. [42] investigated historical and future precipitation and temperature of Alberta using the Special Report on Emissions Scenarios (A1B, A2, and B1) from an ensemble of GCMs. They found future June-July-August precipitation had downward and temperature had upward trends. The magnitude of precipitation and temperature are close to our findings. Zhang et al. [4] also found similar results for Alberta at their Canada-wide study for the historical period of the 20th century. These changes of temperature and precipitation are attributed, at least in part, to the increasing atmospheric greenhouse gases concentration which is mainly due to anthropogenic activities [11,47].

Trend analysis of other hydrological variables in a changing climate is vital to assess climate changes and suggests appropriate water resource management strategies, especially in the agricultural region for the future. Trend analysis of ET, SM, DA, and WYLD are given in Table 4 for the seven counties, and results of these variables are somewhat similar for both RCPs. ET showed a non-significant decreasing trend in all counties during His period, and this trend continued in the future. However, there was a positive trend for annual ET in Grande Prairie county. Similar to the temperature, the trend magnitude of annual ET was higher than that of seasonal magnitudes during the His, NF, and FF. The annual SM during His period showed a decreasing trend in most of the counties except Leduc and Red Deer. For seasonal SM in the His period, most of the counties showed positive trend except Grande Prairie and Mountain View, where the trend was negative. In the future, the annual SM showed a negative trend for both RCPs. In contrast, the seasonal trend in the future was found to be positive for most of the counties. There were some counties which observed a statistically significant trend in annual and seasonal SM for RCP 8.5 only, including Lethbridge (annual SM), Red Deer and Vermilion (seasonal SM). The trend magnitude of DA was very mild. The slope was zero for some of the counties and time horizons. These results indicate a relatively constant level of DA with respect to other hydrological variables during the study periods. In all time periods (His, NF and FF), Grande Prairie showed a non-significant negative trend of DA. Seasonal and annual WYLD trends showed a positive magnitude in most of the counties during the His period (Table 4).

Table 3. Trend of annual and seasonal precipitation and temperature in historic (His: 1983–2007), near future (NF: 2010–2034) and far future (FF: 2040–2064) periods.

		RCP 2.6						RCP 8.5					
		Annual			Seasonal			Annual			Seasonal		
	County	His	NF	FF	His	NF	FF	His	NF	FF	His	NF	FF
		Trend Magnitude											
Precipitation	Ag Region	−0.37	−0.05	−0.17	−0.02	0.00	0.09	−0.37	−0.20	−0.26	−0.02	−0.07	0.00
	Grande Prairie	−1.73	−1.82	−1.90	−2.50 *	−2.36 *	−2.29	−1.73	−1.77	−1.46	−2.50 *	−2.29	−2.32
	Lac Ste. Anne	−3.21	−2.84	−3.25	−2.83	−2.75	−2.92	−3.21	−2.92	−2.96	−2.83	−2.58	−2.83
	Leduc	−0.23	−0.68	−0.34	−2.12	−2.13	−2.04	−0.23	0.23	−0.54	−2.12	−1.65	−2.29
	Vermilion	−0.59	−0.39	−0.22	−0.12	0.38	0.39	−0.59	−0.58	−0.50	−0.12	−0.32	0.29
	Lethbridge	−0.26	−0.50	−0.32	1.36	1.26	1.52	−0.26	−0.36	−0.18	1.36	0.85	1.24
	Mountain View	−0.49	0.16	0.18	−0.34	−0.44	−0.20	−0.49	−0.42	0.01	−0.34	−0.53	−0.40
	Red Deer	−0.07	0.46	0.88	0.34	0.23	0.19	−0.07	0.37	0.71	0.34	−0.10	0.50
Tmean	Ag Region	0.04	0.04	0.04	0.02	0.02	0.02	0.04	0.04	0.04	0.02	0.02	0.02
	Grande Prairie	0.04	0.04	0.04	0.02	0.02	0.02	0.04	0.04	0.04	0.02	0.02	0.01
	Lac Ste. Anne	0.03	0.03	0.03	0.01	0.01	0.01	0.03	0.03	0.03	0.01	0.01	0.01
	Leduc	0.03	0.03	0.03	0.01	0.01	0.01	0.03	0.03	0.03	0.01	0.01	0.01
	Vermilion	0.04	0.04	0.04	0.01	0.02	0.02	0.04	0.04	0.04	0.01	0.02	0.02
	Lethbridge	0.04	0.05	0.04	0.01	0.01	0.01	0.04	0.05	0.04	0.01	0.01	0.01
	Mountain View	0.05 *	0.05	0.05	0.02	0.02	0.02	0.05 *	0.05 *	0.05 *	0.02	0.02	0.02
	Red Deer	0.04	0.04	0.04	0.01	0.01	0.01	0.04	0.04	0.04	0.01	0.01	0.01
Tmax	Ag Region	0.03	0.03	0.03	0.01	0.01	0.01	0.03	0.03	0.03	0.01	0.01	0.01
	Grande Prairie	0.04	0.04	0.04	0.01	0.01	0.01	0.04	0.04	0.04	0.01	0.01	0.01
	Lac Ste. Anne	0.03	0.03	0.03	0.01	0.01	0.01	0.03	0.03	0.03	0.01	0.01	0.01
	Leduc	0.02	0.02	0.02	0.00	0.00	0.00	0.02	0.02	0.02	0.00	0.00	0.00
	Vermilion	0.02	0.02	0.02	−0.02	−0.02	−0.02	0.02	0.02	0.02	−0.02	−0.02	−0.02
	Lethbridge	0.04	0.04	0.04	0.00	0.00	0.00	0.04	0.04	0.04	0.00	0.00	0.00
	Mountain View	0.03	0.03	0.03	0.01	0.01	0.01	0.03	0.03	0.03	0.01	0.01	0.01
	Red Deer	0.03	0.03	0.03	0.01	0.00	0.01	0.03	0.03	0.03	0.01	0.00	0.01
Tmin	Ag Region	0.05	0.05	0.05	0.03	0.03	0.03	0.05	0.05	0.05	0.03	0.03	0.03
	Grande Prairie	0.05	0.05	0.05	0.03	0.02	0.02	0.05	0.05	0.05	0.03	0.02	0.02
	Lac Ste. Anne	0.03 *	0.03	0.03 *	0.03	0.03	0.03	0.03 *	0.03 *	0.03 *	0.03	0.03	0.03
	Leduc	0.05	0.04	0.04	0.02	0.02	0.02	0.05	0.04	0.04	0.02	0.02	0.02
	Vermilion	0.07	0.07 *	0.07	0.04	0.04	0.04	0.07	0.07 *	0.07	0.04	0.03	0.03
	Lethbridge	0.05	0.04	0.05	0.03	0.03	0.03	0.05	0.04	0.05	0.03	0.03	0.03
	Mountain View	0.06 *	0.06 *	0.06 *	0.02	0.02	0.02	0.06 *	0.06 *	0.06 *	0.02	0.02	0.02
	Red Deer	0.05 *	0.04	0.04 *	0.02	0.03	0.03	0.05 *	0.04	0.04 *	0.02	0.03	0.03

* indicates statistically significant at $\alpha = 0.05$. 'Ag Region' indicates the entire study area.

Table 4. Trend of annual and seasonal evapotranspiration (ET), soil moisture (SM), deep aquifer recharge (DA) and water yield (WYLD) in historic (His: 1983–2007), near future (NF: 2010–2034) and far future (FF: 2040–2064).

		RCP 2.6						**RCP 8.5**					
		Annual			**Seasonal**			**Annual**			**Seasonal**		
	County	**His**	**NF**	**FF**	**His**	**NF**	**FF**	**His**	**NF**	**FF**	**His**	**NF**	**FF**
		Trend Magnitude											
ET	Ag Region	−0.03	−0.01	−0.001	0.03	0.03	0.01	−0.03	0.00	−0.007	0.03	0.06	0.01
	Grande Prairie	0.04	0.36	0.28	0.10	0.29	−0.14	0.04	0.38	0.63	0.10	0.31	−0.13
	Lac Ste. Anne	−0.11	−1.21	−1.08	−0.14	−0.91	−0.73	−0.11	−1.27	−1.15	−0.14	−0.93	−0.81
	Leduc	−0.12	−1.68	−1.41	−0.16	−0.78	−0.88	−0.12	−1.54	−1.4	−0.16	−0.60	−0.65
	Vermilion	−0.10	−0.18	−0.72	−0.16	−0.17	−0.40	−0.10	−0.22	−1.51	−0.16	0.01	−1.13
	Lethbridge	−0.12	−2.03	−1.48	−0.18	−2.04	−1.37	−0.12	−0.27	0.13	−0.18	−0.03	0.53
	Mountain View	−0.05	0.40	−0.29	0.07	−0.08	0.41	−0.05	−0.57	−0.41	0.07	−0.02	0.15
	Red Deer	−0.06	−0.41	−0.31	0.00	0.20	0.08	−0.06	−0.62	−0.76	0.00	−0.18	−0.73
SM	Ag Region	0.07	0.16	0.30	0.46	0.43	0.64 *	0.07	0.08	0.43	0.46	0.38	0.70 *
	Grande Prairie	−0.54	−0.65	−0.67	−0.26	−0.19	−0.15	−0.54	−0.96	−0.52	−0.26	−0.16	−0.07
	Lac Ste. Anne	−0.62	−0.72	−0.89	0.04	0.00	0.15	−0.62	−0.48	−0.67	0.04	−0.10	0.01
	Leduc	0.10	−0.74	−0.12	0.06	0.12	0.18	0.10	−0.59	−0.17	0.06	0.10	0.01
	Vermilion	−0.04	−0.94	−0.64	0.53	0.03	0.51 *	−0.04	−0.71	−0.99	0.53	0.05	0.30
	Lethbridge	−0.31	−0.99	−1.03 *	0.13	−0.06	0.07	−0.31	−0.78	−1.26	0.13	0.15	0.14
	Mountain View	−0.22	−0.90	−0.39	−0.10	−0.36	−0.09	−0.22	−0.79	−0.17	−0.10	−0.38	−0.01
	Red Deer	0.74	−0.13	−0.10	0.85	0.57	0.50	0.74	0.01	0.58	0.85	0.51	1.24 *
DA	Ag Region	0.00	0.00	0.001	0.00	0.001	0.003	0.00	0.00	0.002	0.00	0.001	0.004
	Grande Prairie	0.00	−0.05	−0.03	−0.005	−0.03	−0.02	0.00	−0.05	−0.04	−0.005	−0.04	−0.02
	Lac Ste. Anne	0.00	−0.01	0.04	0.00	0.00	0.02	0.00	0.00	0.04	0.00	0.00	0.01
	Leduc	0.00	0.02	0.04	0.002	0.02	0.03	0.00	0.01	0.04	0.002	0.02	0.03
	Vermilion	0.00	0.00	0.01	0.00	0.00	0.01	0.00	0.00	0.01	0.00	0.00	0.01
	Lethbridge	0.00	0.04	0.04	0.008	0.04 *	0.05 *	0.00	0.00	0.02	0.008	0.00	0.03 *
	Mountain View	0.00	0.00	−0.01	0.001	0.00	0.00	0.00	−0.01	0.00	0.001	0.00	0.04
	Red Deer	0.00	0.00	0.01	0.00	0.00	0.00	0.00	0.00	0.06 *	0.00	0.00	0.02
WYLD	Ag Region	0.01	0.005	0.04	0.05	0.04	0.06	0.01	−0.009	0.03	0.05	0.03	0.10
	Grande Prairie	−0.03	−0.29	0.33	0.00	−0.03	−0.02	−0.03	0.17	0.31	0.00	−0.04	−0.02
	Lac Ste. Anne	−0.08	−0.26	0.18	−0.15	0.00	0.02	−0.08	−0.31	−0.08	−0.15	0.00	0.01
	Leduc	0.06	0.98	1.49 *	0.15	0.02	0.03	0.06	0.84	2.71 *	0.15	0.02	0.03
	Vermilion	0.01	0.77	1.48 *	0.03	0.00	0.01	0.01	0.96	2.22	0.03	0.00	0.01
	Lethbridge	0.02	0.13	0.23	0.03	0.04 *	0.05 *	0.02	0.07	0.16	0.03	0.00	0.03 *
	Mountain View	−0.01	−0.05	0.07	0.00	0.00	0.00	−0.01	−0.14	0.48	0.00	0.00	0.04
	Red Deer	0.06	1.17	1.14	0.10	0.00	0.00	0.06	0.90	1.46	0.10	0.00	0.02

* indicates statistically significant at $\alpha = 0.05$. 'Ag Region' indicates the entire study area.

3.4. Monthly Variation of Hydrological Variables

Figure 7 shows the long-term average monthly variation of hydrological variables. The results showed that monthly precipitation, temperature, ET, and SM had a distinct and similar pattern for current and future periods. Precipitation, temperature, and ET followed the bell-shaped curve with the maximum during the agricultural growing season (May-August). Precipitation was projected to increase during the winter and spring seasons (December to May). However, it was likely to show a mixed pattern for the summer and fall seasons (June to November). Projected changes showed a likely uniform increase in temperature throughout the year (Figure 7). Overall, ET was likely to increase and decrease in the ascending and recession limbs of the bell-shaped curve, respectively except for Lethbridge county (Figure 7). SM was projected to decrease in all selected counties except in Lac Ste. Anne and Lethbridge where it was projected to increase concerning the historical. This might be the results of complex in-situ interaction of other hydrological variables such as precipitation, temperature, and ET. Overall, monthly SM is likely to decrease in the future at the scale of entire agricultural region, except in the RCP 8.5 scenario where the results showed an increasing SM. Monthly DA and WYLD were expected to increase in the future, except in Lac Ste. Anne and Lethbridge where monthly variations showed a mixed pattern (Figure S5).

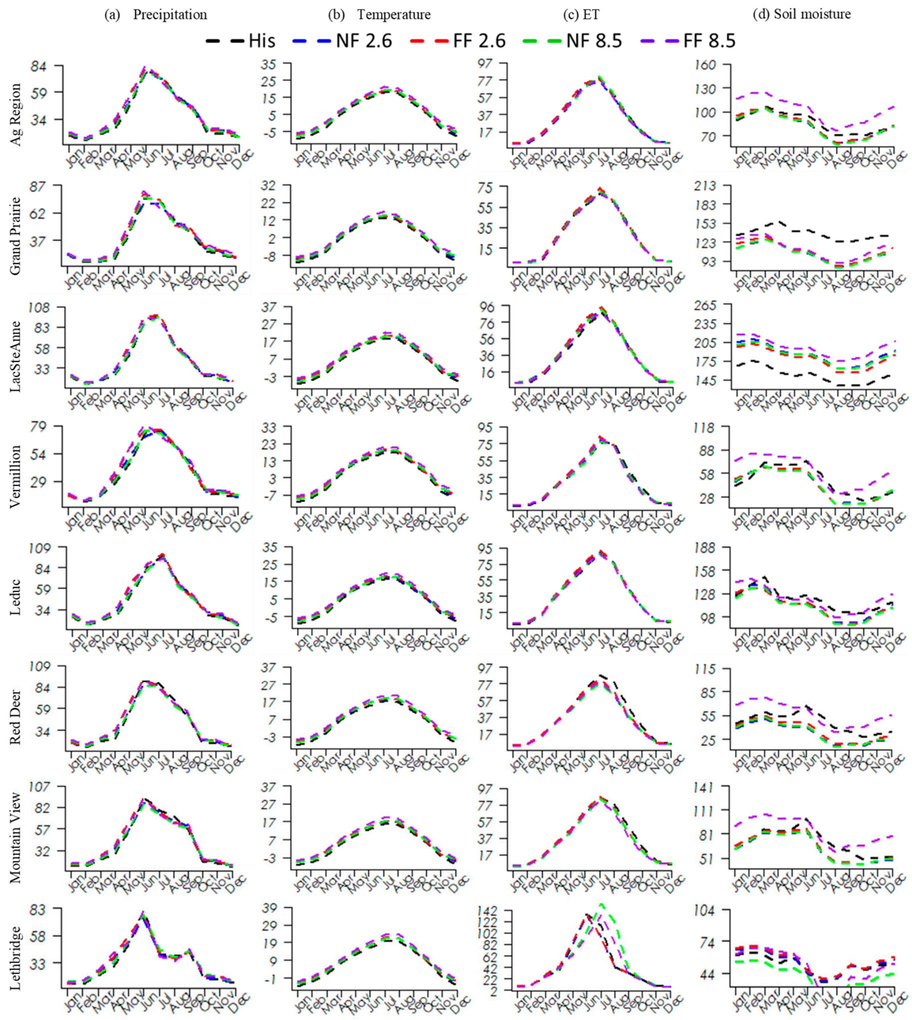

Figure 7. Long-term average monthly (**a**) precipitation, (**b**) temperature (**c**) evapotranspiration (ET), and (**d**) soil moisture in the study area and seven selected counties. 'Ag Region' indicates the entire study area.

3.5. Implications for Agriculture

We compared ET for seven selected counties under two land use conditions (ET_DLU and ET_barley) to analyze their water demand and water deficits. We considered ET as the consumptive water use of plants, and WD as water deficit in the soil that is meant to be compensated by irrigation from other sources (i.e., precipitation minus ET) allowing the plants to reach their actual yields (e.g., barley) or biomass production (e.g., DLU). Figure 8 demonstrates both ET and WD for the selected counties. In a semi-arid region, where agriculture is not the primary land use type, this ET and WD comparison creates useful information to convert the land use for a suitable agricultural crop instead of DLU; in turn, may help to feed growing population. However, we may need to consider the environmental consequences of converting land use types. Because, the change in land use type can alter the atmospheric concentration of CO_2, the principal heat-trapping gas and local climate by changing the energy balance [48]. The WD results showed an apparent pattern for all counties with a negligible WD during May and June, and a considerable amount in July and August for some counties. The maximum negative WD was found in Lethbridge County, indicating a large soil water deficit for the growing season of plants (e.g., barley and DLU) for this county. This result was expected, since historically the Lethbridge County receives less precipitation with high temperature, and most water needs of crop are supplied from irrigation. This information about the ET and WD for DLU and barley (as an example) may help agricultural managers and planners to adopt different strategies to cope with climate change.

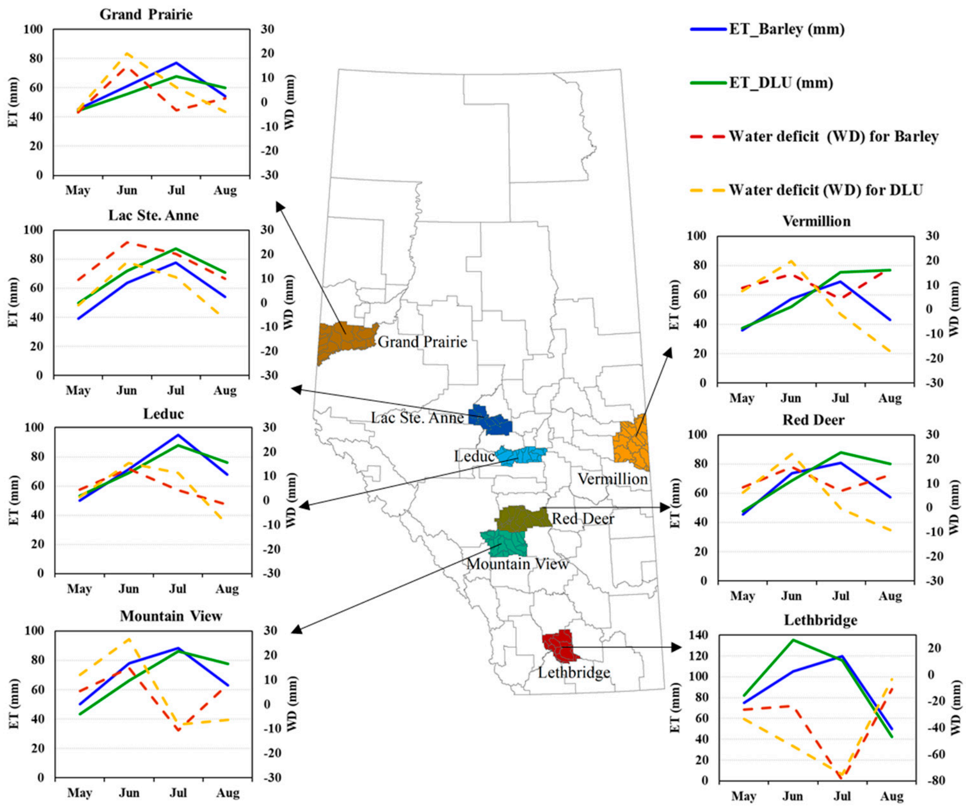

Figure 8. Comparison of evapotranspiration (ET) for dominant land use (DLU) and barley in seven selected counties for the historical 1983–2007 period. Water deficit (WD), which is calculated as the difference in between precipitation and ET for DLU, is also shown in the secondary y-axis.

Increased food demand due to a growing population has to be met by agriculture intensification [49]. Climate change is posing a major challenge to the agricultural sector through increasing concentration of greenhouse gases [3]. In the agriculture sector, climate change may lead to a major shift and extension of croplands favoring proper environment for water demand of crop growths.

Results of this study showed clear evidence of increasing temperature in the Alberta agricultural region. This rising temperature trend could increase the risk of plant diseases, insects infestations, and invasive weeds [50]. Warming temperature also results in longer frost-free seasons which is undoubtedly favorable for the Alberta agriculture. However, the extreme temperature could increase the likelihood of heat-wave related reduction in crop production and consequently in other agricultural industry such as beef-cattle and milk production in the dairy industries in Alberta.

4. Conclusions

Hydrological variables (temperature, precipitation, ET, SM, DA, and WYLD) were analyzed for seasonal and annual variations for the historical (His: 1983–2007) and future (NF: 2010–2034 and FF: 2040–2064) periods.

- Results revealed that the climate in the agricultural region of Alberta had become warmer and drier during the His period. The climate condition is expected to be similar in future periods. Seasonal and annual precipitation is expected to increase by 1% and 3% in the NF while they are projected to increase by 5% and 7% in the FF. The mean seasonal and annual temperature is likely to increase by 1.21 and 1.33 °C in the NF while they are expected an increase by 2.14 and 2.32 °C in the FF, respectively. ET and SM distribution in the future has a resemblance with temperature and precipitation distribution. For instance, a region with high temperature is projected to have high ET and low SM. The blue water resources (DA and WYLD) is likely to increase in the future.
- Trend analysis showed that magnitude of increase and decrease in seasonal precipitation is higher than that of annual precipitation. Mean temperature generally has a higher trend magnitude in the southern part than the north, and a region with a low mean temperature has a higher warming rate. ET shows decreasing trends in the historical as well as in the future periods. SM does not indicate an apparent trend to conclude in the selected counties. However, it is likely to have an increasing trend for the study area. DA and WYLD show very mild trend both in the historical and future periods.
- Long-term average monthly variation of precipitation is expected to increase in winter and spring seasons. The temperature is likely to increase all the year round. ET is expected to increase and decrease in the ascending and recession limbs of the bell-shaped curve having the peak in July. The SM is projected to decrease considering the entire agricultural region, while blue water resources are projected to increase in the future.
- Comparison of water demand (ET) and water deficit (WD) for DLU and barley (as an example crop) indicated that there was no water deficit in May and June, while water deficit existed in July and August in some counties during the His period, that was compensated by irrigation.

It is noteworthy that the causes behind the changes of hydrological variables such as increasing atmospheric greenhouse gases due to anthropogenic actions, natural climate variability, and the effect of management and dam operations on water availability were not explicitly addressed in this study. The results of trend analysis could be influenced by the time period used for the analysis. Hence, the results need to be interpreted carefully. However, the information on projected changes will undoubtedly be useful in adaptation-related decision-making.

Supplementary Materials: The following are available online at http://www.mdpi.com/2073-4441/10/12/1810/s1, The following are available at the supplementary material: Figure S1: Spatial distribution of maximum temperature under RCP 2.6 and 8.5 scenarios, where His indicates historical period (1983–2007), NF indicates near future (2010–2034), and FF indicates far future (2040–2064). For historical period simulated temperature is shown in the map, and for the NF and FF difference of temperature is shown on the map, Figure S2: Spatial distribution of minimum temperature under RCP 2.6 and 8.5 scenarios, where His indicates historical period (1983–2007), NF indicates near future (2010–2034), and FF indicates far future (2040–2064). For historical period simulated temperature is shown in the map, and for the NF and FF difference of temperature is shown on the map, Figure S3: Spatial distribution of deep aquifer recharge under RCP 2.6 and 8.5 scenarios, where His indicates historical period (1983–2007), NF indicates near future (2010–2034), and FF indicates far future (2040–2064). For historical period simulated DA is shown in the map, and for the NF and FF difference of DA is shown in the map, Figure S4: Spatial distribution of water yield under RCP 2.6 and 8.5 scenarios, where His indicates historical period (1983–2007), NF indicates near future (2010–2034), and FF indicates far future (2040–2064). For the historical period simulated WYLD is shown in the map, and for the NF and FF difference of WYLD is shown in the map, Figure S5: Long-term average monthly (a) deep aquifer recharge and (b) water yield in the study area and seven selected counties.

Author Contributions: Conceptualization, M.B.M., J.F. and M.F.; methodology, M.B.M., J.F. and M.F.; formal analysis, M.B.M. and J.F.; data curation, M.B.M., J.F. and M.F.; writing—original draft preparation, M.B.M. and J.F.; writing—review and editing, M.B.M., J.F. and M.F.; visualization, M.B.M. and J.F.; supervision, M.F.

Funding: We gratefully acknowledge the funding from Alberta Agriculture and Forestry (Grant #2016E017R) and the grant awarded by Campus Alberta Innovation Program (Grant #RES0030781).

Conflicts of Interest: The authors declare no conflicts of interest.

References

1. Diffenbaugh, N.S.; Swain, D.L.; Touma, D. Anthropogenic warming has increased drought risk in California. *Proc. Natl. Acad. Sci. USA* **2015**, *112*, 3931–3936. [CrossRef] [PubMed]
2. Piao, S.; Ciais, P.; Huang, Y.; Shen, Z.; Peng, S.; Li, J.; Zhou, L.; Liu, H.; Ma, Y.; Ding, Y.; et al. The impacts of climate change on water resources and agriculture in China. *Nature* **2010**, *467*, 43–51. [CrossRef] [PubMed]
3. IPCC Summary for Policymakers. *Climate Change 2013: Physical Science Basis. Contribution of Working Group I to Fifth Assessment Report of the Intergovernmental Panel Climate Chang*; Cambridge University Press: Cambridge, UK, 2013; Volume 33.
4. Zhang, X.; Vincent, L.A.; Hogg, W.D.; Niitsoo, A. Temperature and precipitation trends in Canada during the 20th century. *Atmosphere-Ocean* **2000**, *38*, 395–429. [CrossRef]
5. Yao, J.; Chen, Y. Trend analysis of temperature and precipitation in the Syr Darya Basin in Central Asia. *Theor. Appl. Climatol.* **2015**, *120*, 521–531. [CrossRef]
6. Chattopadhyay, S.; Edwards, D. Long-term trend analysis of precipitation and air temperature for Kentucky, United States. *Climate* **2016**, *4*, 10. [CrossRef]
7. Hadi, S.J.; Tombul, M. Long-term spatiotemporal trend analysis of precipitation and temperature over Turkey. *Meteorol. Appl.* **2018**, *25*, 445–455. [CrossRef]
8. Zhao, P.; Jones, P.; Cao, L.; Yan, Z.; Zha, S.; Zhu, Y.; Yu, Y.; Tang, G. Trend of surface air temperature in Eastern China and associated large-scale climate variability over the Last 100 Years. *J. Clim.* **2014**, *27*, 4693–4703. [CrossRef]
9. Philandras, C.M.; Nastos, P.T.; Kapsomenakis, J.; Douvis, K.C.; Tselioudis, G.; Zerefos, C.S. Long term precipitation trends and variability within the Mediterranean region. *Nat. Hazards Earth Syst. Sci.* **2011**, *11*, 3235–3250. [CrossRef]
10. Machiwal, D.; Gupta, A.; Jha, M.K.; Kamble, T. Analysis of trend in temperature and rainfall time series of an Indian arid region: Comparative evaluation of salient techniques. *Theor. Appl. Climatol.* **2018**, 1–20. [CrossRef]
11. Vincent, L.A.; Zhang, X.; Brown, R.D.; Feng, Y.; Mekis, E.; Milewska, E.J.; Wan, H.; Wang, X.L. Observed trends in Canada's climate and influence of low-frequency variability modes. *J. Clim.* **2015**, *28*, 4545–4560. [CrossRef]
12. Mekis, É.; Vincent, L.A. An overview of the second generation adjusted daily precipitation dataset for trend analysis in Canada. *Atmosphere-Ocean* **2011**, *49*, 163–177. [CrossRef]
13. Zhang, X.; Harvey, K.D.; Hogg, W.D.; Yuzyk, T.R. Trends in Canadian streamflow. *Water Resour. Res.* **2001**, *37*, 987–998. [CrossRef]
14. Ghafouri-Azar, M.; Bae, D.-H.; Kang, S.-U. Trend analysis of long-term reference evapotranspiration and its components over the Korean Peninsula. *Water* **2018**, *10*, 1373. [CrossRef]
15. Chen, Y.; Guan, Y.; Shao, G.; Zhang, D. Investigating trends in streamflow and precipitation in Huangfuchuan Basin with wavelet analysis and the Mann-Kendall Test. *Water* **2016**, *8*, 77. [CrossRef]
16. Seneka, M.; Figliuzzi, S.J. *Alberta Environment. Trends in Historical Annual Flows for Major Rivers in Alberta*; Alberta Environment: Alberta, VR, USA, 2004; ISBN 0778531929.
17. Jin, H.; Zhu, Q.; Zhao, X.; Zhang, Y. Simulation and prediction of climate variability and assessment of the response of water resources in a typical watershed in China. *Water* **2016**, *8*, 490. [CrossRef]

18. Mehan, S.; Kannan, N.; Neupane, R.; McDaniel, R.; Kumar, S. Climate change impacts on the hydrological processes of a small agricultural watershed. *Climate* **2016**, *4*, 56. [CrossRef]
19. Arias, R.; Rodríguez-Blanco, M.; Taboada-Castro, M.; Nunes, J.; Keizer, J.; Taboada-Castro, M. Water resources response to changes in temperature, rainfall and CO_2 concentration: A first approach in NW Spain. *Water* **2014**, *6*, 3049–3067. [CrossRef]
20. Faramarzi, M.; Abbaspour, K.C.; Adamowicz, W.L.; Lu, W.; Fennell, J.; Zehnder, A.J.B.; Goss, G.G. Uncertainty based assessment of dynamic freshwater scarcity in semi-arid watersheds of Alberta, Canada. *J. Hydrol. Reg. Stud.* **2017**, *9*, 48–68. [CrossRef]
21. Masud, M.B.; Mcallister, T.; Cordeiro, M.R.C.; Faramarzi, M. Modeling future water footprint of barley production in Alberta, Canada: Implications for water use and yields to 2064. *Sci. Total Environ.* **2018**, *616–617*, 208–222. [CrossRef]
22. Cannon, A.J. Selecting GCM scenarios that span the range of changes in a multimodel ensemble: Application to CMIP5 climate extremes indices. *J. Clim.* **2015**, *28*, 1260–1267. [CrossRef]
23. Faramarzi, M.; Srinivasan, R.; Iravani, M.; Bladon, K.D.; Abbaspour, K.C.; Zehnder, A.J.B.; Goss, G.G. Setting up a hydrological model of Alberta: Data discrimination analyses prior to calibration. *Environ. Model. Softw.* **2015**, *74*, 48–65. [CrossRef]
24. Environment and Climate Change Canada. *Climate Data and Scenarios for Canada: Synthesis of Recent Observation and Modelling Results*; Environment and Climate Change Canada: Gatineau, QC, Canada, 2016.
25. Flato, G.; Marotzke, J.; Abiodun, B.; Braconnot, P.; Chou, S.C.; Collins, W.; Cox, P.; Driouech, F.; Emori, S.; Eyring, V.; et al. Evaluation of Climate Models. In *Climate Change 2013: The Physical Science Basis*; Stocker, T.F., Ed.; Cambridge University Press: Cambridge, UK; New York, NY, USA, 2013.
26. Arnold, J.G.; Srinivasan, R.; Muttiah, R.S.; Williams, J.R. Large area hydrologic modeling and assessment Part 1: Model development. *J. Am. Water Resour. Assoc.* **1998**, *34*, 73–89. [CrossRef]
27. Shekhar, S.; Xiong, H. Soil and Water Assessment Tool "SWAT.". *Encycl. GIS* **2008**, 1068. [CrossRef]
28. Neitsch, S.; Arnold, J.; Kiniry, J.; Williams, J. Soil & water assessment tool theoretical documentation version 2009. *Texas Water Resour. Inst.* **2011**, 1–647.
29. Jarvis, A.; Reuter, H.I.; Nelson, A.; Guevara, E. Hole-filled SRTM for the Globe Version 4, the CGIAR-CSI SRTM 90m Database. Available online: http://srtm.csi.cgiar.org/ (accessed on 28 June 2018).
30. Schulze, R. Approaches towards practical adaptive management options for selected water-related sectors in South Africa in a context of climate change. *Water* **2011**, *37*, 621–646. [CrossRef]
31. Mosase, E.; Ahiablame, L. Rainfall and Temperature in the Limpopo River Basin, Southern Africa: Means, Variations, and Trends from 1979 to 2013. *Water* **2018**, *10*, 364. [CrossRef]
32. Kendall, M.G.; Maurice, G.; Gibbons, J.D. *Rank Correlation Methods*; Arnold, E., Ed.; John Wiley & Sons, Inc.: Hoboken, NJ, USA, 1990; ISBN 0195208374.
33. Mann, H.B. Nonparametric tests against trend. *Econometrica* **1945**, *13*, 245–259. [CrossRef]
34. Vincent, L.A.; van Wijngaarden, W.A.; Hopkinson, R.; Vincent, L.A.; van Wijngaarden, W.A.; Hopkinson, R. Surface temperature and humidity trends in Canada for 1953–2005. *J. Clim.* **2007**, *20*, 5100–5113. [CrossRef]
35. Singh, P.; Kumar, V.; Thomas, T.; Arora, M. Changes in rainfall and relative humidity in river basins in northwest and central India. *Hydrol. Process.* **2008**, *22*, 2982–2992. [CrossRef]
36. Masud, M.B.; Soni, P.; Shrestha, S.; Tripathi, N.K. Changes in climate extremes over North Thailand, 1960–2099. *J. Climatol.* **2016**, *2016*, 1–18. [CrossRef]
37. Gedefaw, M.; Wang, H.; Yan, D.; Song, X.; Yan, D.; Dong, G.; Wang, J.; Girma, A.; Ali, B.; Batsuren, D.; et al. Trend analysis of climatic and hydrological variables in the Awash River Basin, Ethiopia. *Water* **2018**, *10*, 1554. [CrossRef]
38. Yue, S.; Pilon, P.; Cavadias, G. Power of the Mann–Kendall and Spearman's rho tests for detecting monotonic trends in hydrological series. *J. Hydrol.* **2002**, *259*, 254–271. [CrossRef]
39. Liu, S.; Huang, S.; Huang, Q.; Xie, Y.; Leng, G.; Luan, J.; Song, X.; Wei, X.; Li, X. Identification of the non-stationarity of extreme precipitation events and correlations with large-scale ocean-atmospheric circulation patterns: A case study in the Wei River Basin, China. *J. Hydrol.* **2017**, *548*, 184–195. [CrossRef]
40. Asong, Z.E.; Khaliq, M.N.; Wheater, H.S. Projected changes in precipitation and temperature over the Canadian Prairie Provinces using the Generalized Linear Model statistical downscaling approach. *J. Hydrol.* **2016**, *539*, 429–446. [CrossRef]

41. Forbes, K.A.; Kienzle, S.W.; Coburn, C.A.; Byrne, J.M.; Rasmussen, J. Simulating the hydrological response to predicted climate change on a watershed in southern Alberta, Canada. *Clim. Chang.* **2011**, *105*. [CrossRef]
42. Jiang, R.; Gan, T.Y.; Xie, J.; Wang, N.; Kuo, C.-C. Historical and potential changes of precipitation and temperature of Alberta subjected to climate change impact: 1900–2100. *Theor. Appl. Clim.* **2017**, *127*, 725–739. [CrossRef]
43. Kienzle, S.W.; Nemeth, M.W.; Byrne, J.M.; MacDonald, R.J. Simulating the hydrological impacts of climate change in the upper North Saskatchewan River basin, Alberta, Canada. *J. Hydrol.* **2012**, *412–413*, 76–89. [CrossRef]
44. Schindler, D.W.; Donahue, W.F. An impending water crisis in Canada's western prairie provinces. *Proc. Natl. Acad. Sci. USA* **2006**, *103*, 7210–7216. [CrossRef]
45. Farjad, B.; Gupta, A.; Marceau, D.J. Annual and seasonal variations of hydrological processes under climate change scenarios in two sub-catchments of a complex watershed. *Water Resour. Manag.* **2016**, *30*, 2851–2865. [CrossRef]
46. Falkenmark, M.; Rockström, J. The new blue and green water paradigm: Breaking new ground for water resources planning and management. *J. Water Resour. Plan. Manag.* **2006**, *132*, 129–132. [CrossRef]
47. Zhang, X.; Zwiers, F.W.; Stott, P.A.; Zhang, X.; Zwiers, F.W.; Stott, P.A. Multimodel multisignal climate change detection at regional scale. *J. Clim.* **2006**, *19*, 4294–4307. [CrossRef]
48. Marland, G.; Pielke, R.A.; Apps, M.; Avissar, R.; Betts, R.A.; Davis, K.J.; Frumhoff, P.C.; Jackson, S.T.; Joyce, L.A.; Kauppi, P.; et al. The climatic impacts of land surface change and carbon management, and the implications for climate-change mitigation policy. *Clim. Policy* **2003**, *3*, 149–157. [CrossRef]
49. Lindemann, T.; Morra, D. Climate change: Implications on agriculture and food security in the short-medium term. In *Global Warming and Climate Change*; Palgrave Macmillan UK: London, UK, 2010; pp. 78–96.
50. Pathak, T.; Maskey, M.; Dahlberg, J.; Kearns, F.; Bali, K.; Zaccaria, D. Climate change trends and impacts on California agriculture: A Detailed review. *Agronomy* **2018**, *8*, 25. [CrossRef]

© 2018 by the authors. Licensee MDPI, Basel, Switzerland. This article is an open access article distributed under the terms and conditions of the Creative Commons Attribution (CC BY) license (http://creativecommons.org/licenses/by/4.0/).